Taylor & Francis
Taylor & Francis Group

Tunnelling, non-collinearity and current-induced switching in metal/heterojunctions

P. WEINBERGER*

Center for Computational Materials Science, Gumpendorferstr. 1a,
A-1060 Vienna, Austria

Current-induced switching in heterojunctions such as Fe/Vac/Fe and Fe/Ge/Fe, including in the latter case homogeneous and inhomogeneous chemical disorder caused by holes (vacuum), is described theoretically in terms of a multi-scale approach based on *ab initio* calculations using the fully relativistic screened Korringa–Kohn–Rostoker method and the Landau–Lifshitz–Gilbert equation. It is found that (1) the presence of tunnelling can be a function of the relative angle between the orientations of the magnetization in the magnetic slabs; and (2) disorder is responsible for the occurrence of non-collinear magnetic ground states. Furthermore, it is found that the first terms in the expansion of the twisting energy in a power series in the cosine of this relative angle, namely the interlayer exchange energy term and the anisotropy term, can be used for a qualitative scheme not only to characterize the occurrence of non-collinear ground states, but also for the critical current needed to induce switching.

1. Introduction

Current-induced switching in spin valve type systems appears, as originally suggested theoretically by Slonczewski [1], to have become a prominent topic in spintronics (see, for example, [2]), since, in 'traditional' magnetic devices or media, the magnetic moments are switched via externally generated magnetic fields and not, as suggested simply by applying a current pulse perpendicularly through the magnetic layers itself. In this context the question has frequently been posed whether or not current-induced switching would also be possible for heterojunctions, i.e. in systems with a non-metallic spacer. Although this partially leads back to the problems encountered experimentally and theoretically when using so-called semi-conducting spacers or non-conducting spacer materials such as metal oxides, the prospect of current-induced 'tunnelling' is quite intriguing, in particular if the critical current necessary to switch the magnetic moments can be substantially reduced.

An approach is presented based on previous experience in dealing with heterojunctions [3–8] (for reviews, see, e.g., [9, 10]) and a recently proposed scheme [11] to correlate *ab initio* calculated sheet resistances and twisting energies with the current required to induce the switching, both being based on the concept of non-collinear

---

*Email: pw@cms.tuwien.ac.at

magnetic configurations. In order to illustrate the various features to be seen in the case of heterojunctions, two types of systems were considered, namely vacuum and Ge as spacer materials. Furthermore, since a realistic non-metallic spacer material can show structural disorder, this was simulated by considering two types of chemical disorder by means of the statistical distribution of 'holes' either homogeneously or inhomogeneously in a Ge spacer in terms of the Coherent Potential Approximation [12, 13]. Clearly, using vacuum as a spacer is a kind of academic exercise, which, however, is quite illustrative for showing the establishment of 'tunnelling'. Disorder, on the other hand, can create non-collinear (magnetic) ground states, the interplay between 'tunnelling' and non-collinear ground states therefore being perhaps the main feature to be encountered in current-induced switching in heterojunctions. Whether or not heterojunctions can serve as current-induced switching devices will in the first place depend on how well interdiffusion at the interfaces and the structural properties of the spacer can be controlled experimentally. Viewed in this context the present paper can only hint at the actual difficulties to be met.

The paper is organized as follows. First, theoretical concepts such as non-collinear magnetic structures, twisting energies, sheet resistances, currents and switching times are briefly summarized. In this section a qualitative condition for the occurrence of 'tunnelling' is also given using complex Fermi energies. In the subsequent section the results for the various types of spacers considered are presented. Finally, in the last section an attempt is made to classify the occurrence of non-collinear (magnetic) ground states and the critical current in terms of an expansion for the twisting energy, in which the first terms correspond to the well-known interlayer exchange energy and the anisotropy energy.

2. Theoretical concepts

If within the (non-relativistic) Density Functional Theory (DFT) $G(z)$ denotes the resolvent of the Kohn–Sham–Dirac Hamiltonian,

$$G(z) = (z - \mathcal{H})^{-1}, \quad z = \epsilon + i\delta,$$

then within the Kubo–Greenwood equation [10] the diagonal elements of the conductivity tensor are defined as

$$\sigma_{\mu\mu} = \frac{\hbar}{\pi N_0 \Omega_{\text{at}}} \text{tr}\langle J_\mu \text{Im}G^+(\epsilon_{\text{F}}) J_\mu \text{Im}G^+(\epsilon_{\text{F}})\rangle, \tag{1}$$

where $\text{Im}G^+(\epsilon)$,

$$\text{Im}G^+(\epsilon) = \frac{1}{2i}(G^+(\epsilon) - G^-(\epsilon)),$$

can be formulated in terms of the so-called side-limits of $G(z)$,

$$\lim_{|\delta| \to 0} G(z) = \begin{cases} G^+(\epsilon), & \delta > 0, \\ G^-(\epsilon), & \delta < 0. \end{cases}$$

Usually, multiple scattering theory [13] is applied in order to evaluate $G(z)$ in the configuration space representation (Green's function) and to perform the trace in equation (1). If the system under consideration can be characterized by two-dimensional translational symmetry (a layered system; one and the same translational invariance has to apply in all atomic layers) then for a particular magnetic configuration $\mathcal{C}$ the diagonal elements of the conductivity tensor can be written [10, 12] as a double sum over atomic layers,

$$\sigma_{\mu\mu}(\mathcal{C}; N) = \frac{1}{N} \sum_{p,q=1}^{N} \sigma_{\mu\mu}^{pq}(\mathcal{C}; N),$$

where

$$\sigma_{\mu\mu}^{pq}(\mathcal{C}; N) = \lim_{\delta \to 0} \sigma_{\mu\mu}^{pq}(\mathcal{C}; N; \delta), \tag{2}$$

$$\sigma_{\mu\mu}^{pq}(\mathcal{C}; N; \delta) = \frac{1}{4} \sum_{i,j=1}^{2} (-1)^{i+j} \sigma_{\mu\mu}^{pq}(\mathcal{C}; \epsilon_i, \epsilon_j; N),$$

$$\epsilon_i, \epsilon_j = \epsilon_F \pm i\delta,$$

and N denotes the total number of atomic layers taken into account.

2.1. *Non-collinear magnetic structures*

In principle, in a layered system a different orientation of the magnetization can apply in each atomic layer. Let $\mathbf{n}_i$ denote the orientations in the individual layers and $\mathbf{n}_L$ and $\mathbf{n}_R$ the orientation of the (possibly magnetic) semi-infinite substrate and the semi-infinite top, then a typical non-collinear magnetic configuration is defined by

$$\mathcal{C} = \{\mathbf{n}_L, \mathbf{n}_1, \ldots, \mathbf{n}_N, \mathbf{n}_R\}.$$

Furthermore, let $\mathbf{n}_0$ point along the surface normal and $\mathbf{n}_0'$ be rotated continuously around an axis perpendicular to the surface normal by an angle $\Theta \in [0, \pi]$. Now consider a magnetic configuration in which $\mathbf{n}_L$ and $\mathbf{n}_i$, $i \le N/2$, are parallel to $\mathbf{n}_0$, and $\mathbf{n}_L$ and $\mathbf{n}_i$, $i > N/2$, are parallel to $\mathbf{n}_0'$, then obviously in order to characterize such a configuration it is sufficient to supply only the angle Θ, i.e. $\mathcal{C}$ is completely specified by Θ. The parallel magnetic configuration then corresponds to $\Theta = 0$, and the antiparallel one to $\Theta = \pi$. As in the following systems of the type Fe/spacer/Fe with a non-magnetic spacer are considered, all investigations are restricted to this type of non-collinear magnetic configuration.

2.2. *Twisting energies*

Define the so-called twisting energy [11] $\Delta E(\Theta; m)$ as follows:

$$\Delta E(\Theta; m) = E(\Theta; m) - \min[E(\Theta; m)], \tag{3}$$

where, for simplicity, m denotes the number of spacer layers; this quantity is positive definite for all Θ. It should be noted that the difference $E(\pi; m) - E(0; m)$ is nothing

but the well-known interlayer exchange coupling energy, which specifies whether the coupling of two magnetic slabs separated by a non-magnetic spacer is parallel (ferromagnetic) or antiparallel (antiferromagnetic). The energy $\Delta E(\Theta; m)$ has to be regarded as a kind of excitation energy, which, for example by means of an external magnetic field, has to be supplied in order to move the system from the ground state, $\min[E(\Theta; m)]$, to a state referring to a different, in general non-collinear, magnetic configuration.

Furthermore, since, in principle, in the case of heterojunctions the spacer can be inhomogeneously disordered, in the following notation $\Delta E(\Theta; \mathbf{x}, m)$ is generally used, where $\mathbf{x}$ is an m-dimensional vector whose elements specify the concentrations of two chosen constituents in each spacer layer. In the case of a homogeneous alloy forming the spacer $\mathbf{x} = x\mathbf{I}$, $\mathbf{I} = (1, 1, \ldots, 1)$, for an ordered system $\mathbf{x} = \mathbf{I}$. If interdiffusion occurs at the interfaces between the magnetic slabs and the spacer then $\mathbf{x}$ has to also include a few layers of the magnetic slabs.

2.3. *Sheet resistances*

Making use of complex Fermi energies, $\mathcal{E}_F = \epsilon_F \pm i\delta$, then according to equation (2) the sheet resistance for a given magnetic configuration characterized by a particular value of Θ is defined by

$$r(\Theta; \mathbf{x}, m) = \lim_{\delta \to 0} r(\Theta, \delta; \mathbf{x}, m), \qquad (4)$$

where

$$r(\Theta, \delta; \mathbf{x}, m) = \sum_{i,j=1}^{N} \rho_{ij}(\Theta, \delta; \mathbf{x}, m),$$

$$\sum_{k=1}^{N} \rho_{ik}(\Theta, \delta; \mathbf{x}, m)\sigma_{kj}(\Theta, \delta; \mathbf{x}, m) = \delta_{ij},$$

and N consists of m spacer layers and a sufficient number of layers of the lead material. In the present investigations, 12 Fe layers were included on each side of the spacer, i.e. $N = m + 24$. The sheet resistance $r(\Theta; \mathbf{x}, m)$ is related to the resistance $R(\Theta; \mathbf{x}, m)$ via the relation $r(\Theta; \mathbf{x}, m) = A_0 R(\Theta; \mathbf{x}, m)$, in which A_0 denotes the unit area, and to $\rho_{\text{CPP}}(\Theta; \mathbf{x}, m)$, the resistivity in the current perpendicular to the planes of atoms geometry (CPP), via $r(\Theta; \mathbf{x}, m) = L\rho_{\text{CPP}}(\Theta; \mathbf{x}, m)$, where L is the overall length of the structure for which the conductivity is calculated.

2.4. *Physical significance of the imaginary part of the Fermi energy*

Suppose that, in the Kubo–Greenwood equation (see equation (1)), the current operator can be approximated by a constant,

$$\bar{\sigma} \sim \text{tr}\langle \text{Im}G^+(\epsilon_F)\text{Im}G^+(\epsilon_F)\rangle \sim n^2(\epsilon_F), \qquad (5)$$

which, in turn, implies that the sheet resistance can approximately be written as

$$\bar{r} = L\bar{\rho} = L\bar{\sigma}^{-1} = Ln^{-2}(\epsilon_F).$$

Furthermore, suppose the density of states $n(\epsilon_F)$ in equation (5) is calculated using complex Fermi energies, $\mathcal{E}_F = \epsilon_F + i\delta$, $\delta > 0$,

$$\bar{r}(\delta) = L/\bar{\sigma}(\delta) = Ln^{-2}(\epsilon_F + i\delta).$$

Then from the properties of the density of states,

$$\frac{d[n(\epsilon_F + i\delta)]}{d\delta} = \begin{cases} > 0, & \text{'non-metallic',} \\ < 0, & \text{'metallic',} \end{cases}$$

it follows immediately that

$$\frac{d[\bar{r}(\delta)]}{d\delta} = \begin{cases} > 0, & \text{'metallic',} \\ < 0, & \text{'non-metallic'.} \end{cases}$$

The functional form of the actually calculated sheet resistance with respect to the imaginary part of the Fermi energy can therefore be used to qualitatively interpret the underlying type of conductance

$$\frac{d[r(\Theta; \mathbf{x}, m; \delta)]}{d\delta} = \begin{cases} > 0, & \text{'metallic',} \\ < 0, & \text{'non-metallic'.} \end{cases} \tag{6}$$

The last equation indicates *inter alia* that, in the case of a negative slope of the sheet resistance with respect to δ, 'tunnelling' might occur. The parameter δ obviously acts as a (small) constant self-energy: in the regime of metallic conductance, an increase in the self-energy implies increased resistivity (sheet resistance); in the non-metallic regime, an increase in δ reduces the resistance, and the system becomes more metallic. Equation (6) will be used to indicate in which system and at what value of Θ 'tunnelling' seems to occur. It turns out that the condition in equation (6) is quite useful, in particular in the case of disordered spacers. However, since this equation only states a qualitative condition, above and in the following the term tunnelling appears within quotation marks.

2.5. *Currents*

The corresponding current $I(\Theta; \mathbf{x}, m)$ can be defined [11] in terms of the twisting energy $\Delta E(\Theta; \mathbf{x}, m)$ (see equation (3)) and the sheet resistance $r(\Theta; \mathbf{x}, m)$,

$$\begin{aligned} I(\Theta; \mathbf{x}, m) &= \sqrt{\frac{A_0 \Delta E(\Theta; \mathbf{x}, m)}{\tau(\Theta; \mathbf{x}, m)r(\Theta; \mathbf{x}, m)}} \\ &= \sqrt{\frac{\langle A_0 \rangle}{\langle \tau(\Theta; \mathbf{x}, m) \rangle}} I_0(\Theta; \mathbf{x}, m), \end{aligned} \tag{7}$$

where $\tau(\Theta; \mathbf{x}, m)$ is the time needed to accomplish such a rotation by Θ. In equation (7), $\langle A_0 \rangle$ and $\langle \tau(\Theta; \mathbf{x}, m) \rangle$ denote the magnitudes of the corresponding quantities within the international system of units; $I_0(\Theta; \mathbf{x}, m)$ will be referred to below as the reduced current, which depends only on the twisting energy and the sheet resistance. At zero temperature (the temperature at which *ab initio* calculations

are performed) the twisting energy corresponds to the free energy such that, to determine the times $\tau(\Theta; \mathbf{x}, m)$, the Landau–Lifshitz–Gilbert equation can be applied using the following kth-order power series in $\cos(\Theta)$:

$$\Delta E^{(k)}(\Theta; \mathbf{x}, m) = \sum_{s=0}^{k} a_s(\mathbf{x}, m)(\cos(\Theta))^s. \tag{8}$$

The only quantity in equation (7) that cannot be determined theoretically is the unit area A_0, since it is an experimental parameter, which, of course, depends very much on the design of the prepared samples.

Finally, let Θ_0 denote the ground state,

$$E(\Theta_0; \mathbf{x}, m) = \min[E(\Theta; \mathbf{x}, m)], \tag{9}$$

then quite obviously

$$I(\Theta_0; \mathbf{x}, m) = 0. \tag{10}$$

The critical current, namely the current that has to be applied to excite the system from a collinear ground state Θ_0 to a collinear final state, can then be defined as

$$I(\Theta_1; \mathbf{x}, m) = \max\{I(\Theta; \mathbf{x}, m)\}$$

$$= \sqrt{\frac{\langle A_0 \rangle}{\langle \tau(\Theta_1; \mathbf{x}, m) \rangle}} I_0(\Theta_1; \mathbf{x}, m), \tag{11}$$

i.e. it refers to the maximal value of $I(\Theta; \mathbf{x}, m)$ with respect to $\Theta \in [0, \pi]$. Below it will be seen that if the (magnetic) ground state refers to a non-collinear configuration Θ_1, then the definition in equation (11) has to be modified.

2.6. *Switching times*

For layered systems (two-dimensional translational invariant systems) the Landau–Lifshitz–Gilbert equation can be written in the following form [11]:

$$\frac{\mathrm{d}\vec{n}}{\mathrm{d}t} = -\gamma \vec{n} \times \mathbf{H}^{\mathrm{eff}}(\mathbf{x}, m) + \alpha \vec{n} \times (\vec{n} \times \mathbf{H}^{\mathrm{eff}}(\mathbf{x}, m)),$$

$$\vec{n} = n_x \mathbf{e}_x + n_y \mathbf{e}_y + n_z \mathbf{e}_z, \tag{12}$$

where γ is the (Gilbert) gyromagnetic ratio, α the dimensionless Gilbert damping parameter, $\mathbf{e}_x$, $\mathbf{e}_y$ and $\mathbf{e}_z$ are unit vectors and $\vec{n}$ refers to the direction of the magnetic moment $\mathbf{M}$ averaged over all layers with magnetic moments $\mathbf{M}_i$ forming the magnetic slab that is rotated,

$$\vec{n} = \frac{\mathbf{M}}{M_0}, \quad \mathbf{M} = \frac{1}{N} \sum_{i=1}^{N} \mathbf{M}_i. \tag{13}$$

It should be noted that, in equations (12) and (13), it is assumed that all moments are uniformly oriented in the rotated part of the system, i.e. they are not only

ferromagnetically ordered within the atomic planes (translational invariance), but also with respect to different planes.

At zero temperature the internal effective field $\mathbf{H}^{\mathrm{eff}}(\mathbf{x}, m)$ in equation (12) can be associated with the change in the total energy $E(\mathbf{x}, m)$ with respect to $\mathbf{M}$,

$$\mathbf{H}^E(\mathbf{x}, m) = -\frac{\partial E(\mathbf{x}, m)}{\partial \mathbf{M}} = -\nabla_{\mathbf{M}} E(\mathbf{x}, m). \tag{14}$$

Restricting the expansion in equation (8) to a third-order series in $\cos \Theta$ and rewriting, for simplicity, the coefficients there as

$$a = -a_1(\mathbf{x}, m), \quad b = a_2(\mathbf{x}, m), \quad c = a_3(\mathbf{x}, m), \tag{15}$$

$$\Delta E(\mathbf{M}; \mathbf{x}, m) \simeq \Delta E^{(3)}(\Theta; \mathbf{x}, m), \tag{16}$$

then, provided that the rotational axis is the x axis ($n_x = 0$),

$$\mathbf{M} \times \mathbf{H}^E(\mathbf{x}, m) = \mathbf{e}_x M_y H_z^E(\mathbf{x}, m)$$
$$= -n_y(-a + 2b\,n_z + 3cn_z^2)\mathbf{e}_x, \tag{17}$$

and

$$\mathbf{M} \times (\mathbf{M} \times \mathbf{H}^E(\mathbf{x}, m)) = -n_y(-a + 2b\,n_z + 3cn_z^2)$$
$$\times (M_z\,\mathbf{e}_y - M_y\,\mathbf{e}_z). \tag{18}$$

Furthermore, since $n_y^2 + n_z^2 = 1$, equation (12) reduces to

$$M_0 \frac{\mathrm{d}n_z}{\mathrm{d}t} = \alpha(1 - n_z^2)(-a + 2b\,n_z + 3cn_z^2), \tag{19}$$

which can be integrated directly assuming that $n_z \neq \pm 1$ or $(-b \pm (b^2 + 3ac)^{1/2})/3c$ and $b^2 + 3ac > 0$, $c \neq 0$. The time τ needed to change n_z from the initial orientation n_z^{i} to the final orientation n_z^{f} is then given [11] by

$$\tau = \frac{M_0}{\alpha}(\tau_1 + \tau_2 + \tau_3), \tag{20}$$

with

$$\tau_1 = \frac{1}{2[(3c - a) - 2b]}\left[\ln\left|\frac{n_z^{\mathrm{f}} + 1}{n_z^{\mathrm{i}} + 1}\right| - \ln\left|\frac{n_z^{\mathrm{f}} - 1}{n_z^{\mathrm{i}} - 1}\right|\right],$$

$$\tau_2 = -\frac{b}{(3c - a)^2 - 4b^2}\ln\left|\frac{3c\left(n_z^{\mathrm{f}}\right)^2 + 2b\,n_z^{\mathrm{f}} - a}{3c\left(n_z^{\mathrm{i}}\right)^2 + 2b\,n_z^{\mathrm{i}} - a}\right|,$$

$$\tau_3 = \left[\frac{1}{(3c-a)^2 - 4b^2} \frac{a(3c-a) + 2b^2}{2\sqrt{b^2 + 3ac}}\right]$$

$$\times \ln\left|\frac{(b + 3cn_z^f) - \sqrt{b^2 + 3ac}}{(b + 3cn_z^i) - \sqrt{b^2 + 3ac}} \times \frac{(b + 3cn_z^i) + \sqrt{b^2 + 3ac}}{(b + 3cn_z^f) + \sqrt{b^2 + 3ac}}\right|.$$

Since, at present, there is no quantum mechanical expression for the damping factor α, in the following the choice $\alpha = 1$ is used. The corresponding switching times will be referred to as the minimal switching time [11]. For bulk Fe the experimental damping factor is about 0.5 [14, 15] and for Fe single films it is 1.5 [16, 17]. Therefore, choosing a damping factor of 1 for Fe heterojunctions would appear to be quite realistic.

3. Computational details

For all systems investigated, the parallel configuration was calculated self-consistently with $\mathbf{n}_0$ pointing along the surface normal by using the fully relativistic Screened Korringa–Kohn–Rostoker method [13] and the density functional para-meterization of Vosko *et al.* [18]. Chemical disorder (the alloy problem) was treated in terms of the (inhomogeneous) Coherent Potential Approximation [13]. The twist-ing energies were then obtained via the magnetic force theorem [19] by calculating the grand potentials $E(\Theta; \mathbf{x}, m)$ [10, 13] in equation (3) using a sufficient number of $\mathbf{k}$ points in the Surface Brillouin zone in order to guarantee stable convergence. The sheet resistances $r(\Theta; \mathbf{x}, m)$ were evaluated in terms of the fully relativistic Kubo–Greenwood equation [10, 12], again using a sufficiently large $\mathbf{k}$ set. In both types of calculations the angle Θ was varied between 0 and $180°$ in steps of $15°$. Layer relaxations were not included in either type of calculation, i.e. in all investi-gated systems the interlayer spacing is uniformly that of bcc Fe, namely $1.3942\,\text{Å}$. The derivative of $\Delta E(\Theta; \mathbf{x}, m)$ with respect to $\cos(\Theta)$ (see equation (8)) was deter-mined numerically by a linear least-squares fitting procedure [20], since then $\tau(\Theta; \mathbf{x}, m)$ can easily be calculated with sufficient accuracy for any value of Θ between 0 and π.

4. Results

4.1. *The system Fe/vacuum/Fe*

Although the system (bcc)-Fe/Vac$_n$/Fe [3] is only academic, it has the advantage that no questions arise concerning the actual structure and composition of the spacer. By considering one to five vacuum layers, the width d of the vacuum barrier changes from about 1.39 to $6.97\,\text{Å}$. From figure 1, showing the sheet resistances $r(\Theta; \delta; \mathbf{x}, m)$ for $\delta = 0$, 2 and 3 mryd displayed versus the rotation angle Θ, it is immediately evident that 'tunnelling' (see equation (6)) not only depends on d, but also on Θ: for $m = 1$ and $m = 3$, 'tunnelling' seems to occur only for Θ greater than about 150 and $120°$, respectively, whereas for $m = 2$ and $m \geq 4$, the sheet resistance $r(\Theta; \delta; \mathbf{x}, m)$ is always larger for $\delta = 0$ than for finite values of δ. This is an interesting observation,
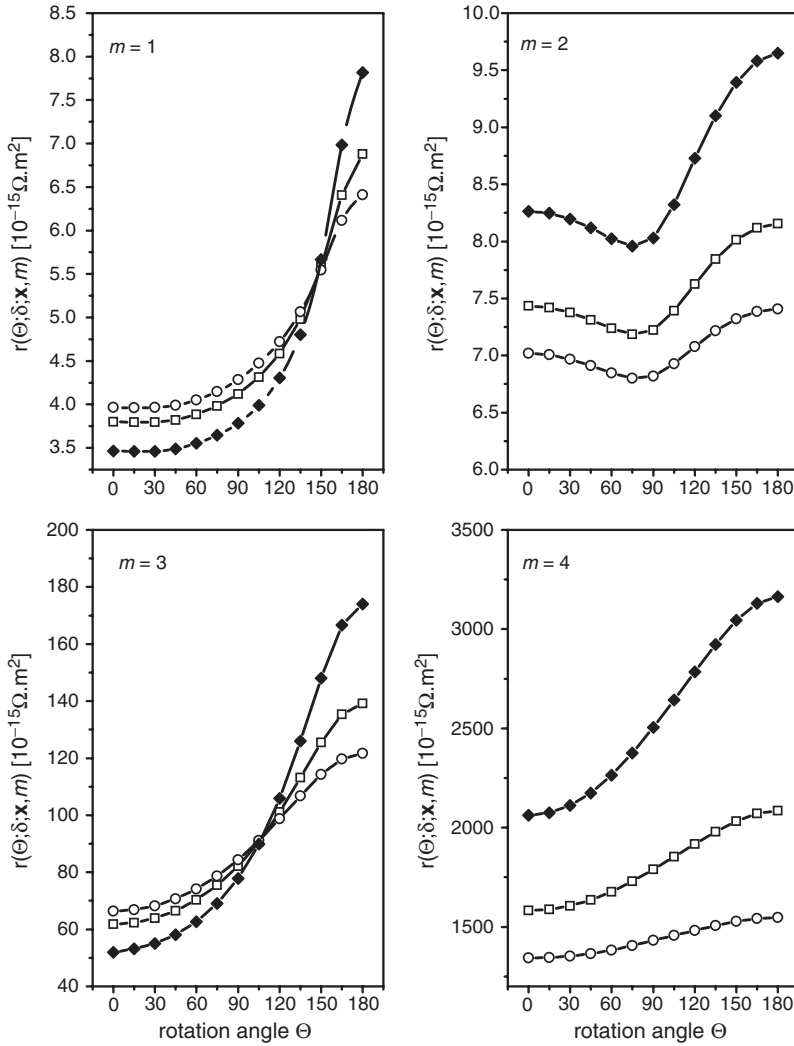
Figure 1. Properties of the sheet resistance $r(\Theta, \delta; \mathbf{x}, m)$ as a function of the rotation angle Θ and the imaginary part δ of the Fermi energy for the system Fe/Vac$_n$/Fe. Full symbols refer to $\delta = 0$, open squares to $\delta = 2$ and open circles to $\delta = 3$ mryd. The number of vacuum layers is shown.

since, in realistic systems, in which the spacer is formed by a material that, as bulk material, is either semi- or non-conducting, a situation similar to the case of $m = 1$ or 3 can occur, caused, for example by finite spacer thicknesses, structural rearrangements, etc.

Figure 2 shows the reduced current $I_0(\Theta; \mathbf{x}, m)$ versus the rotation angle. As can be seen, $I_0(\Theta_1; \mathbf{x}, m)$, the reduced critical current (see equation (11)), does not necessarily correspond to a collinear magnetic configuration. Clearly, since $r(\Theta; \mathbf{x}, m)$ increases dramatically with increasing m, $I_0(\Theta_1; \mathbf{x}, m)$ vanishes rapidly. This is shown
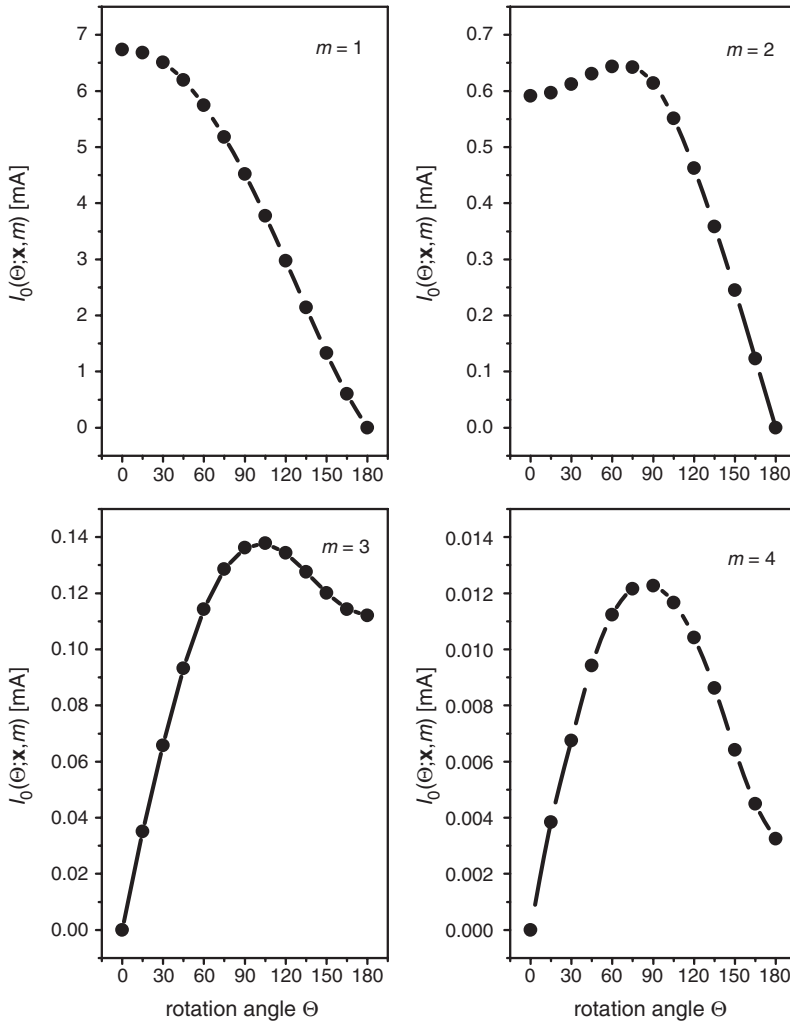
Figure 2. Reduced current $I_0(\Theta; \mathbf{x}, m)$ as a function of the rotation angle Θ for the system Fe/Vac$_n$/Fe. The number of vacuum layers is shown.

in figure 3 together with $\Theta_1(\mathbf{x}, m)$. It should be noted that, for graphical reasons, the sheet resistance in this figure is displayed in units of $10^{-12}\,\Omega\,\mathrm{m}^2$.

4.2. The system Fe/Ge$_\mathbf{m}$/Fe

For the heterojunction bcc-Fe/Ge$_m$/Fe [4], four cases were considered, namely $m = 12$, 15, 18 and 21, thus comprising a range of spacer thicknesses d between 16.73 and 29.28 Å. Figure 4 shows the dependence of the sheet resistance with respect to the imaginary part of the Fermi energy for these four cases versus the rotation angle Θ. As can be seen for all four spacer thicknesses, 'tunnelling' seems to occur
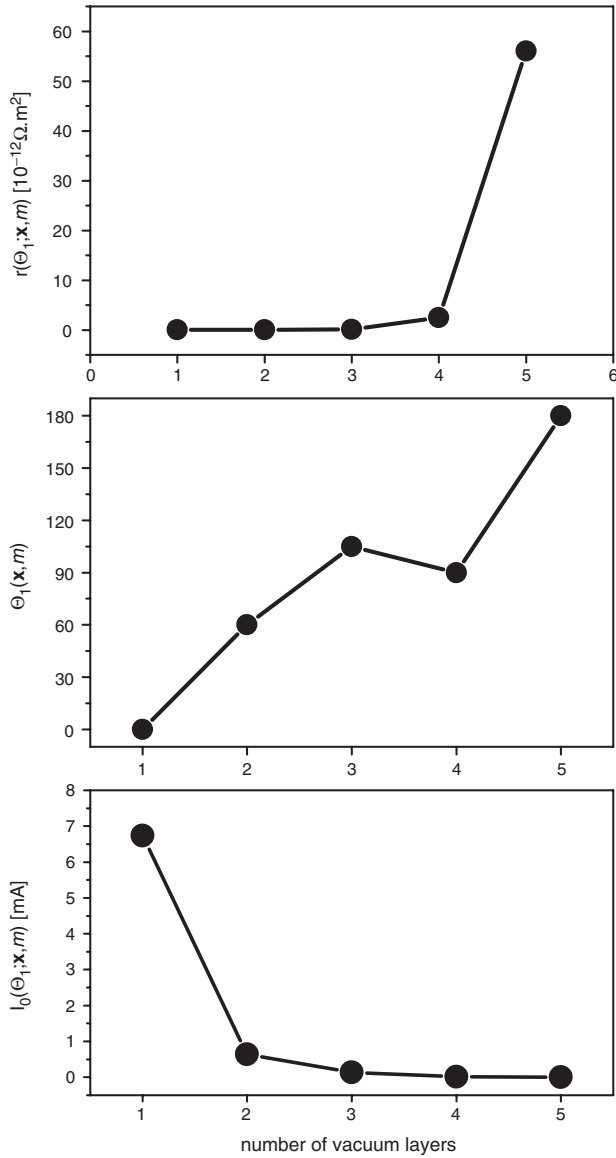
Figure 3. Sheet resistance $r(\Theta_1; \mathbf{x}, m)$, reduced critical current $I_0(\Theta_1; \mathbf{x}, m)$ and $\Theta_1(\mathbf{x}, m)$ versus the number of vacuum layers. Note that the angle $\Theta_1(\mathbf{x}, m)$ characterizes the maximum of $I_0(\Theta_1; \mathbf{x}, m)$ (see equation (11)).

only for values of Θ much greater than $90°$. Inspecting the cross-over point more closely, one can see that, with increasing spacer thickness, this point moves to smaller values of Θ, perhaps indicating that, for a sufficiently thick spacer, 'tunnelling' applies for all values of Θ.

Figure 5 shows the reduced currents for these four cases with respect to Θ, and the corresponding reduced critical currents $I(\Theta_1; \mathbf{x}, m)$ and the respective $\Theta_1(\mathbf{x}, m)$
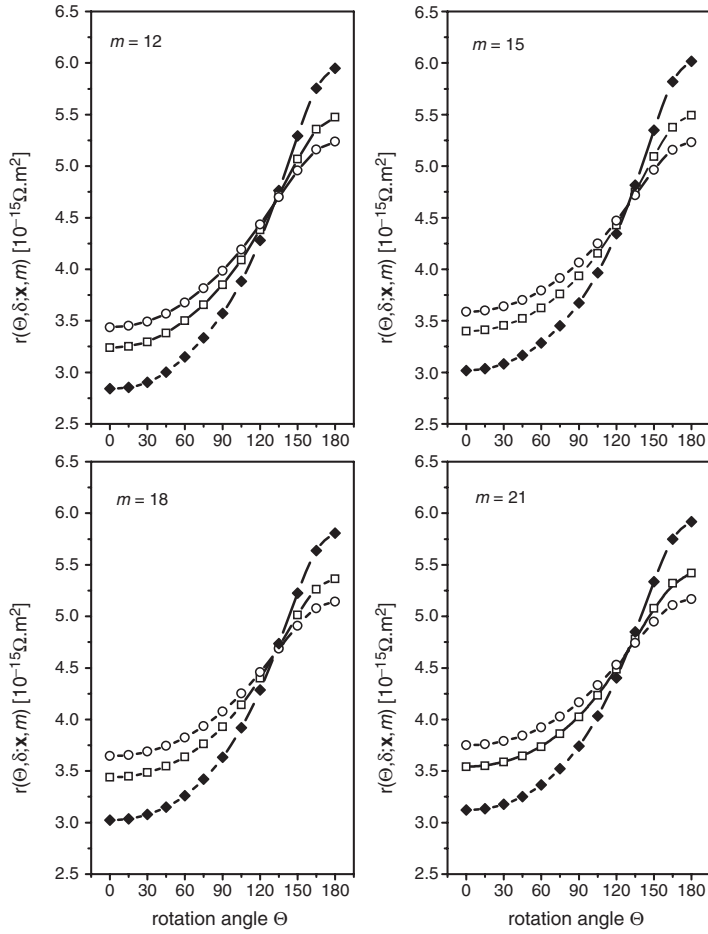
Figure 4. Properties of the sheet resistance $r(\Theta, \delta; \mathbf{x}, m)$ as a function of the rotation angle Θ and the imaginary part δ of the Fermi energy for the system $Fe/Ge_m/Fe$. Full symbols refer to $\delta = 0$, open squares to $\delta = 2$ and open circles to $\delta = 3$ mryd. The number of Ge layers is shown.

values are displayed in figure 6 versus the number of Ge layers. Clearly, $I(\Theta_1; \mathbf{x}, m)$ decreases rapidly with increasing spacer thickness. Surprisingly, however, for $m = 18$ and 21 the value of $\Theta_1(\mathbf{x}, m)$ no longer corresponds to a collinear arrangement. This implies, for example in the case of $m = 21$, that at least $I(\Theta_1; \mathbf{x}, m)$ has to be applied in order to switch the system from the parallel configuration (ground state) to the antiparallel configuration.

4.3. *The system $Fe/(Ge_x Vac_{1-x})_m/Fe$*

Since the actual structure of a spacer in a heterojunction does not necessarily have to follow the stacking sequence of the leads, two different types of disorder were investigated, namely: (a) the case of a homogeneously disordered spacer consisting
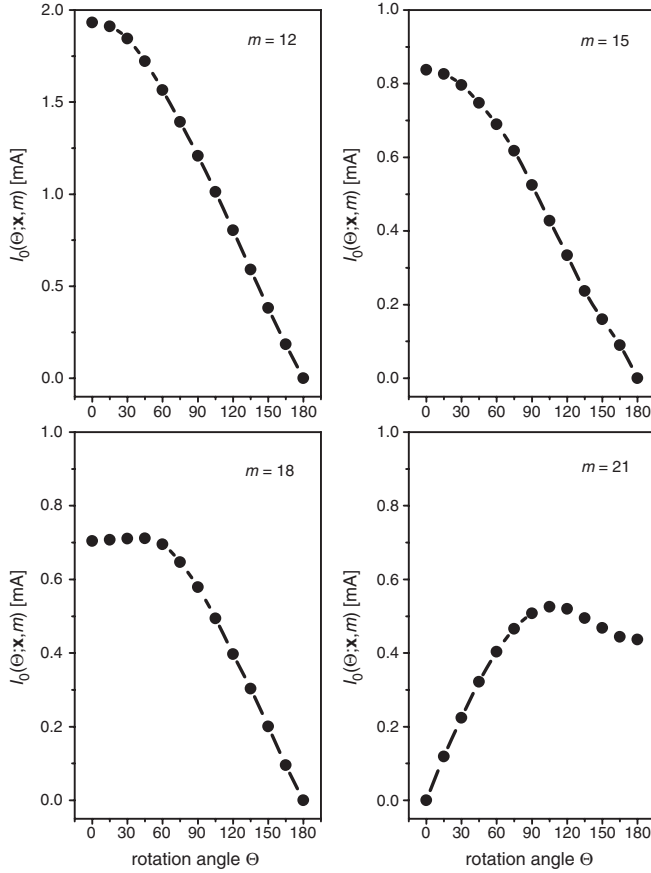
Figure 5. Reduced current $I_0(\Theta; \mathbf{x}, m)$ for Fe/Ge$_m$/Fe, $m = 12$, 15, 18 and 21.

of Ge and 'holes', statistically placed on lattice positions, i.e. for the spacer a disordered 'alloy' of type Ge$_x$Vac$_{1-x}$ was considered [4]; and (b) the case of an inhomogeneously disordered spacer with alternating concentrations [4] (see the following section). Such an approach is particularly appropriate, since very often because of the usual experimental preparation techniques such as sputtering, etc., the actual structure of the spacer is little known.

As an example of the first case, figures 7–9 consider a heterojunction with a spacer consisting of 12 homogeneously disordered atomic layers ($d = 16.73\,\text{Å}$). From the figure displaying the reduced current (figure 7) it is clear that 10% statistically distributed 'holes' is sufficient to cause the system to assume a non-collinear ground state, implying that switching can occur between this state and both collinear magnetic configurations. Therefore, if in equation (9) $\Theta_0 \neq 0, \pi$ then two different times can be distinguished,

$$\tau(\mathbf{x}, m) = \begin{cases} t(0, \Theta_0; \mathbf{x}, m), \\ |t(\Theta_0, \pi; \mathbf{x}, m)|, \end{cases} \tag{21}$$
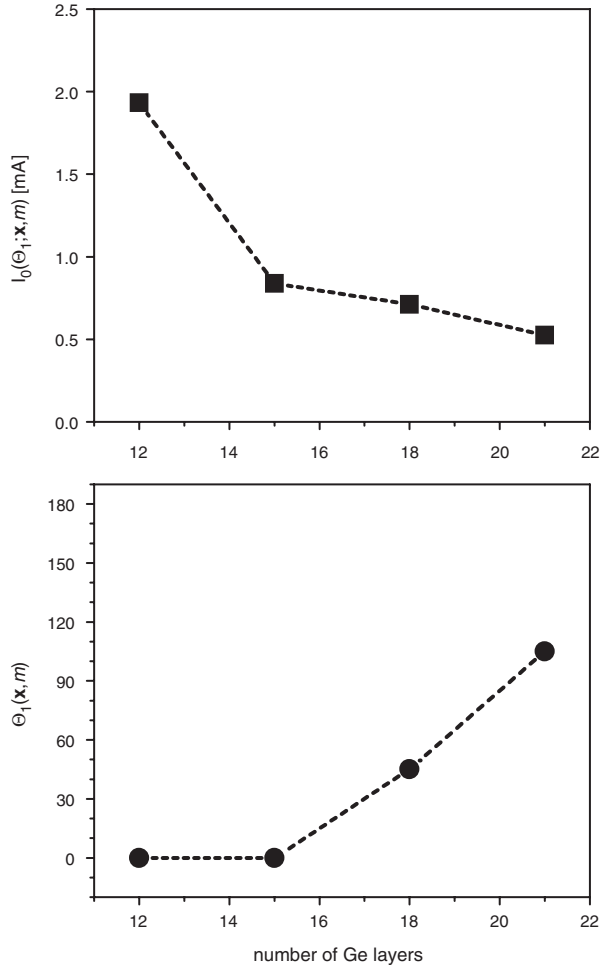
Figure 6.   Reduced critical current $I_0(\Theta_1; \mathbf{x}, m)$ and $\Theta_1(\mathbf{x}, m)$ for the system Fe/Ge$_m$/Fe.

where $t(\Theta_i, \Theta_j; \mathbf{x}, m)$ is the minimal time needed to force the system from the state corresponding to Θ_i into the state corresponding to Θ_j, such that the following convention can be adopted:

$$I(\Theta; \mathbf{x}, m) = \begin{cases} +\sqrt{\langle A_0/\tau(\Theta; \mathbf{x}, m)\rangle} I_0(\Theta; \mathbf{x}, m), & \Theta \leq \Theta_0, \\ -\sqrt{\langle A_0/|\tau(\Theta; \mathbf{x}, m)|\rangle} I_0(\Theta; \mathbf{x}, m), & \Theta \geq \Theta_0, \end{cases}$$

and consequently two different critical currents can be defined,

$$I^+(\Theta_1; \mathbf{x}, m) = \max\{I(\Theta; \mathbf{x}, m) | \Theta \leq \Theta_0\},$$
$$I^-(\Theta_1; \mathbf{x}, m) = \min\{I(\Theta; \mathbf{x}, m) | \Theta \geq \Theta_0\}. \tag{22}$$
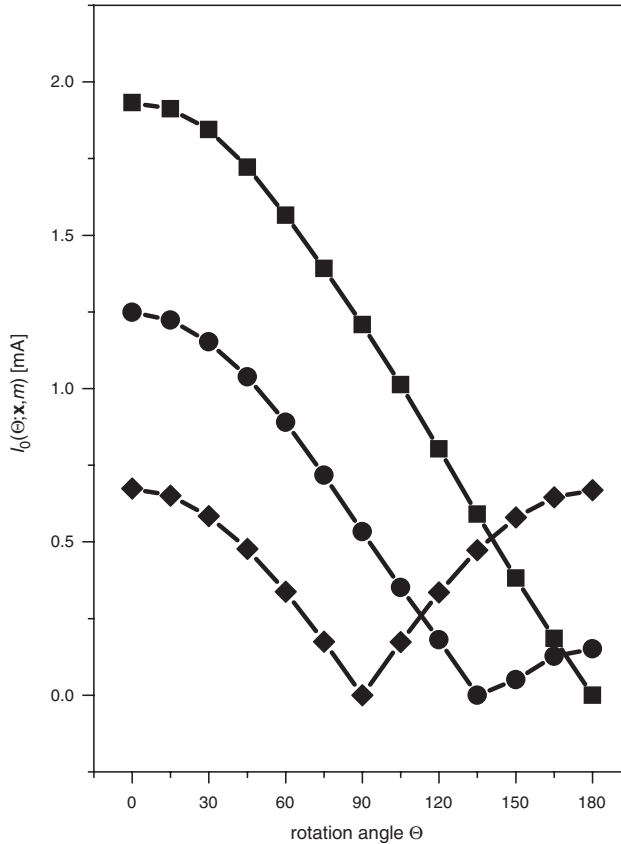
Figure 7. Reduced current $I_0(\Theta; \mathbf{x}, m)$ versus Θ for the heterojunction Fe/Ge/Fe with 12 homogeneously disordered spacer layers for $x = 0.8$ (diamonds), 0.9 (circles) and 1.0 (squares).

Clearly, if $\Theta_0 = 0$ or π, then switching takes place between the two collinear magnetic configurations, one of which is the ground state, and $\Theta_1(\mathbf{x}, m)$ characterizes the maximum of $I(\Theta; \mathbf{x}, m)$ with respect to $\Theta \in [0, \pi]$. If, however, $\Theta_0 \neq 0, \pi$ then two kinds of reduced critical currents $I_0(\Theta_1; \mathbf{x}, m)$ can be distinguished according to the possible intervals $\Theta_1 \in [0, \Theta_0]$ and $\Theta_1 \in [\Theta_0, \pi]$.

This can readily be seen from figure 7, since, for $x = 0.9$, the value of the reduced current at $\Theta = \pi$ is much smaller than at $\Theta = 0$. For $x = 0.8$ (and all concentrations less than 0.8, not shown), Θ_0 is at $\pi/2$ with $I_0(\Theta_1 \leq \pi/2; \mathbf{x}, m)$ and $I_0(\Theta_1 > \pi/2; \mathbf{x}, m)$ being approximately of the same size.

Figure 8 shows the corresponding sheet resistances for different values of δ. It is clear from this figure that a few percent of 'holes' statistically distributed in the spacer is sufficient to destroy the 'tunnelling' properties present in the corresponding ordered spacer for $\Theta > 135°$. With disorder present, metallic-like conductance seems to characterize the electric transport properties of the system. Finally, figure 9 summarizes the situation for a Ge spacer homogeneously disordered by 'holes': the
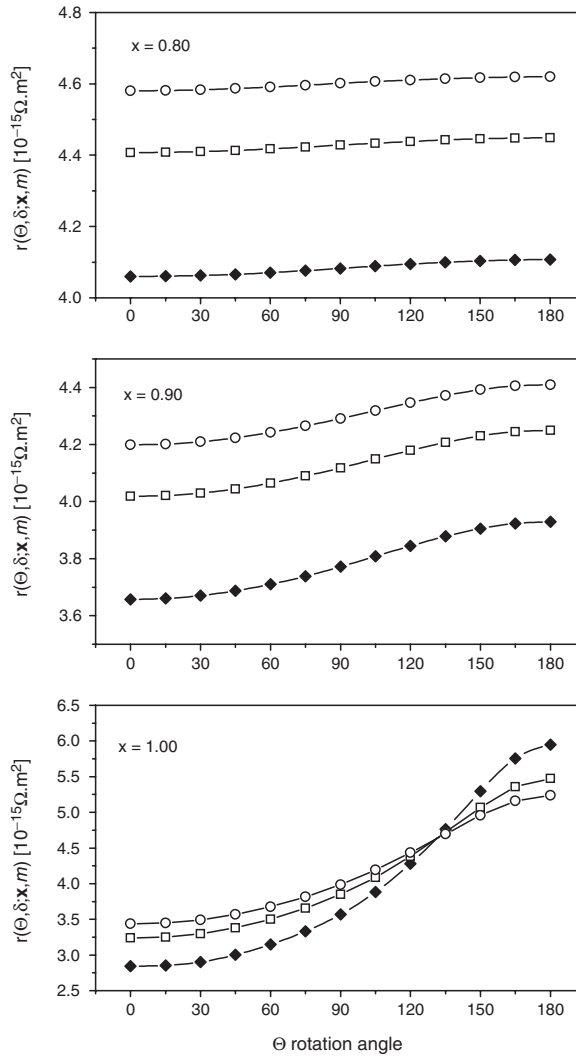
Figure 8.   Properties of the sheet resistance $r(\Theta, \delta; \mathbf{x}, m)$ as a function of Θ and the imaginary part δ of the Fermi energy for the heterojunction Fe/Ge/Fe with 12 homogeneously disordered spacer layers for $x = 0.8$, 0.9 and 1.0. Full symbols refer to $\delta = 0$, open squares to $\delta = 2$ and open circles to $\delta = 3$ mryd.

magnetoresistance (top), defined, in general, as

$$\mathrm{MR}(\Theta; \mathbf{x}, m) = \frac{r(\Theta; \mathbf{x}, m) - r(0; \mathbf{x}, m)}{r(\Theta; \mathbf{x}, m)},$$

at $\Theta = \pi$ immediately decreases from about 50% to only a few percent for $x = 0.9$ and vanishes completely for $x \leq 0.8$. The reduced current at $\Theta = 0$ increases sharply for $x \geq 0.8$, while that at $\Theta = \pi$ drops to zero. It should be recalled from figure 5 that for 12 Ge spacer layers the antiparallel configuration is the ground state.
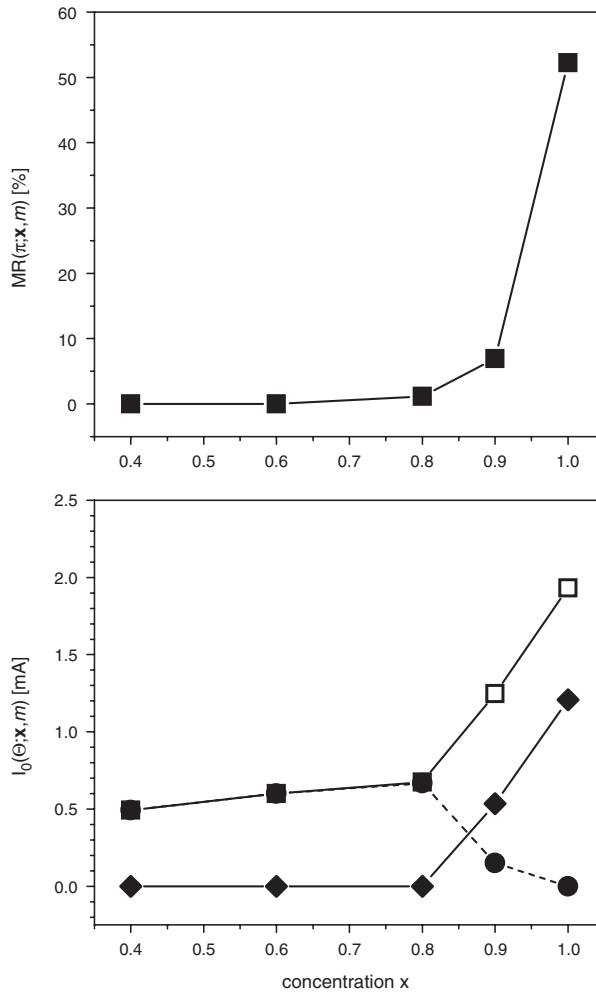
Figure 9. Magnetoresistance MR$(\pi; \mathbf{x}, m)$ (top) and values of the reduced current $I_0(\Theta; \mathbf{x}, m)$ (bottom) for $\Theta = 0$ (open squares), $\pi/2$ (diamonds) and π (circles) versus the concentration x for the system with 12 homogeneously disordered Ge layers.

4.4. *The system Fe/(Ge$_{1-x}$Vac$_x$)(Ge$_x$Vac$_{1-x}$)...(Ge$_{1-x}$Vac$_x$)/Fe*

As the second type of disorder a Ge spacer was chosen with alternating concentrations in 15 layers, namely Fe/(Ge$_{1-x}$Vac$_x$)(Ge$_x$Vac$_{1-x}$)...(Ge$_{1-x}$Vac$_x$)/Fe [4], i.e. an inhomogeneously disordered system ($d = 20.91$ Å). In this particular case the vector $\mathbf{x}$ is defined as $\mathbf{x} = (1 - x, x, 1 - x, x, \ldots, 1 - x)$. Clearly, if $x = 1$ the spacer consists of alternating empty planes and ordered planes of Ge atoms: Fe/Vac/Ge/Vac/$\cdots$/Vac/Fe. For $x = 0.5$, one obtains an equi-concentrational homogeneously disordered system as discussed in the previous section. For $x = 0$, one obtains the other kind of termination, namely the stacking sequence Fe/Ge/Vac/Ge/$\cdots$/Ge/Fe. Only the more interesting cases of $x \geq 0.5$ are investigated here.
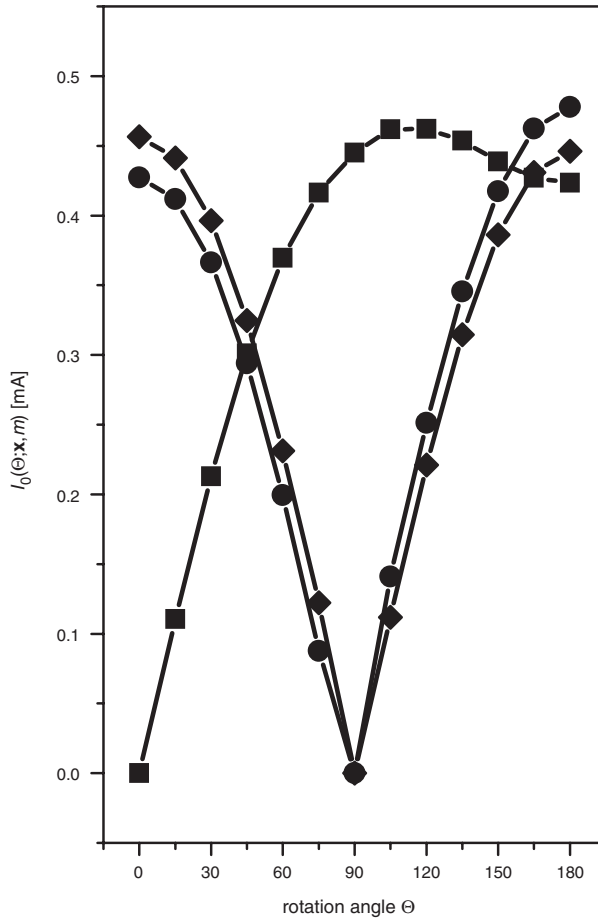
Figure 10. Reduced current $I_0(\Theta; \mathbf{x}, m)$ versus Θ for the heterojunction Fe/Ge/Fe with 15 inhomogeneously disordered Ge layers, $x = 0.8$ (diamonds), 0.9 (circles) and 1.0 (squares).

Figure 10 shows the reduced currents $I_0(\Theta; \mathbf{x}, m)$ for $x = 0.8$, 0.9 and 1.0. As can readily be seen, for $x < 1$ a non-collinear ground state is preferred, while for $x = 1$ the parallel configuration is lowest in energy. Furthermore, for $x = 1$ the reduced current has a maximum that is not located at either $\Theta = 0, \pi$ or $\pi/2$. The sheet resistances in figure 11 demonstrate that, for $x = 1$, 'tunnelling' seems to apply for all values of Θ, which, however, is immediately destroyed on introducing inhomogeneous disorder. For concentrations $x \leq 0.9$, metallic behaviour characterizes the conductance. Finally, figure 12 summarizes the situation for this type of disorder. As can be seen the magnetoresistance at $\Theta = \pi$ immediately decreases almost to zero at $x = 0.9$ and vanishes completely for lower concentrations. The reduced currents at $\Theta = 0$, $\pi/2$ and π show interesting behaviour, since only for $x > 0.8$ do changes occur: the values at $\Theta = 0$ and π show a maximum at about $x = 0.95$ and then drop either to zero ($\Theta = 0$), or ($\Theta = \pi$) are almost identical to that at $\Theta = \pi/2$ (see also figure 10).
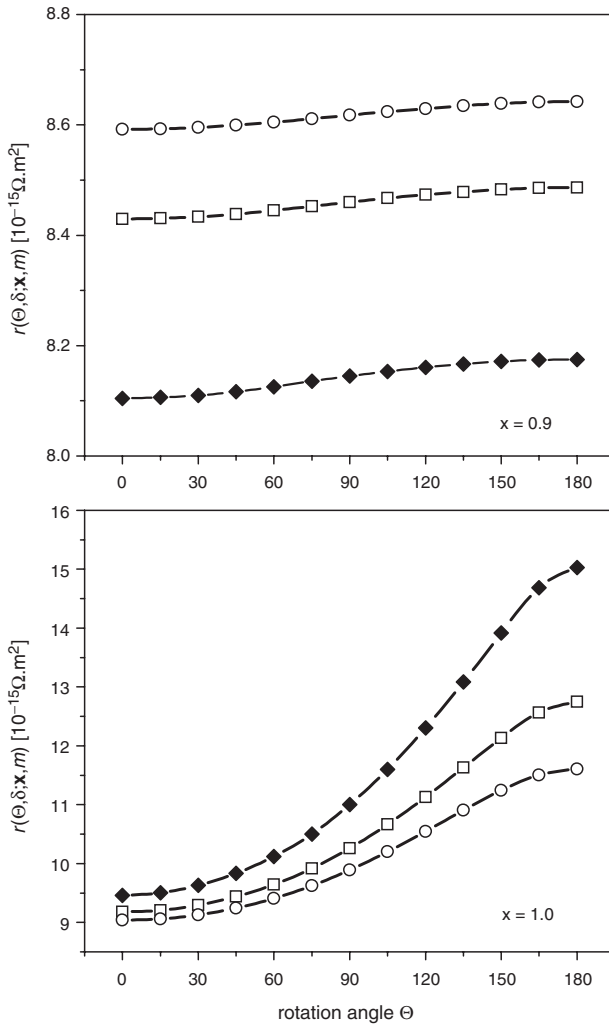
Figure 11. Properties of the sheet resistance $r(\Theta, \delta; \mathbf{x}, m)$ versus Θ for the heterojunction Fe/Ge/Fe with 15 inhomogeneously disordered Ge layers for $x = 0.9$ and 1.0. Full symbols refer to $\delta = 0$, open squares to $\delta = 2$ and open circles to $\delta = 3$ mryd.

4.5. *Switching times*

Figure 13 shows the minimal switching times $t(\Theta_i, \Theta_j; \mathbf{x}, m)$ for the system Fe/Vac$_n$/Fe versus the number of vacuum layers. In order to understand these results properly, it is useful to inspect in figure 14 the variation of the expansion coefficients of $\Delta E(\Theta; \mathbf{x}, m)$ as defined in equation (15), in which, as should be recalled, a corresponds to the (negative) coefficient for $\cos \Theta$, which governs the interlayer exchange term, and b corresponds to that for $\cos^2 \Theta$, i.e. to the anisotropy term. As can be seen from figure 2 for $m = 1, 2$ the ground state corresponds to the antiparallel configuration ($a < 0$), while for $m = 3$ it is the parallel configuration ($a > 0$). For $m \geq 4$
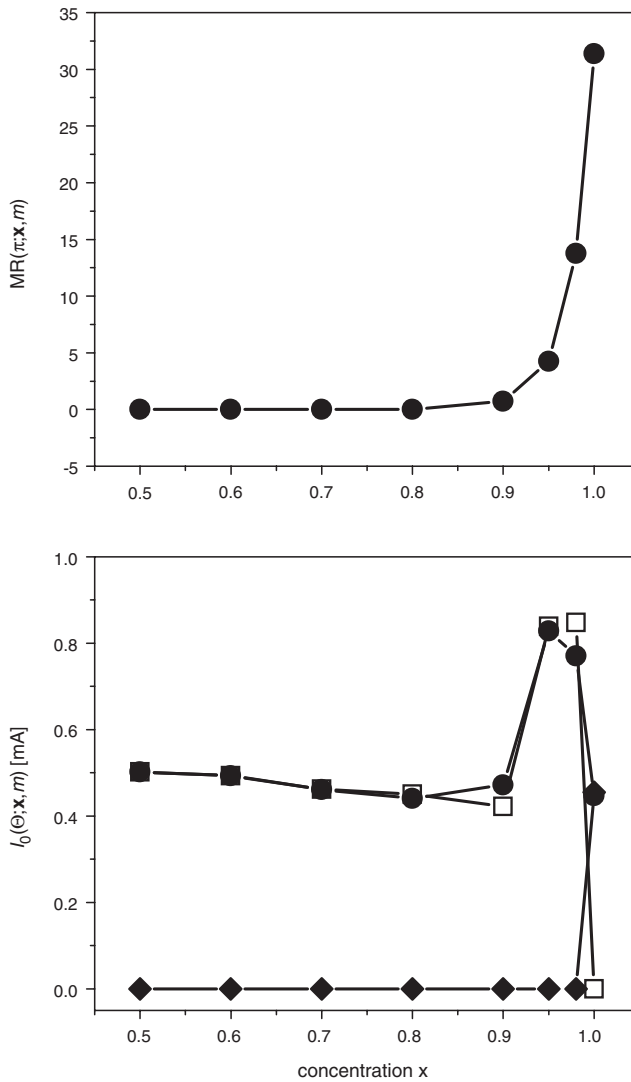
Figure 12. Magnetoresistance $MR(\pi; \mathbf{x}, m)$ (top) and values of the reduced current $I_0(\Theta; \mathbf{x}, m)$ (bottom) for $\Theta = 0$ (open squares), $\pi/2$ (diamonds) and π (circles) versus the concentration x for the heterojunction with 15 homogeneously disordered Ge layers.

the twisting energy is mostly determined by the anisotropy term ($|b| \geq |a|$). The peak in the minimal switching time at $m = 3$ has to be related therefore to the fact that, in this particular case, both a and b are positive and of reasonably large size. This can also be seen from the corresponding entry for $m = 3$ in figure 2, where the reduced current for this case is displayed.

Figures 15 and 16 are particularly interesting, since they show the transition from metallic conductance to tunnelling *and* the transition from a non-collinear ground state to a collinear one in terms of minimal switching times. From figure 7 it is clear
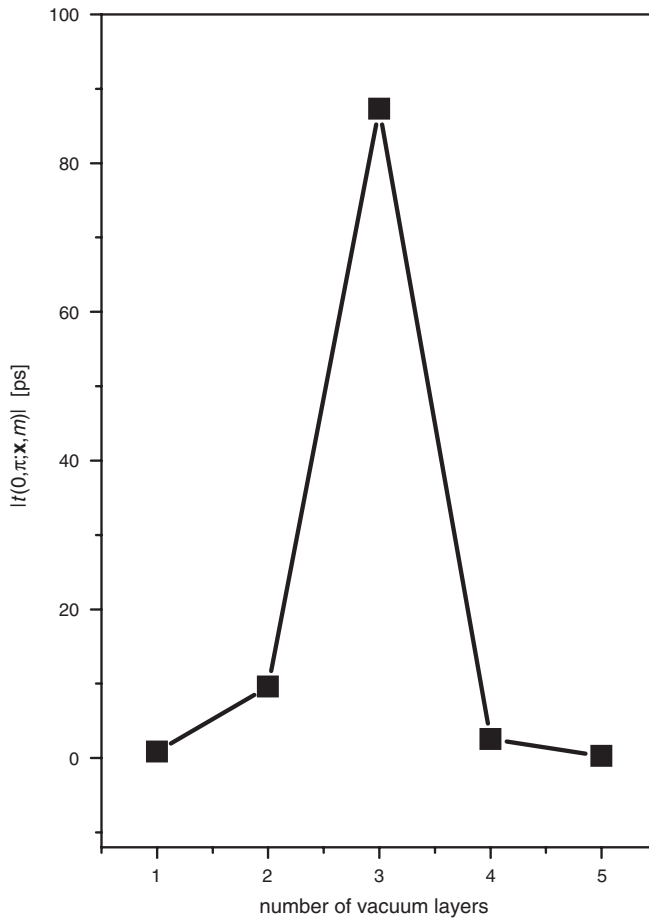
Figure 13. Minimal switching times $|t(0, \pi; \mathbf{x}, m)|$ for the system Fe/Vac$_m$/Fe.

that, in the case of a 12 ML thick homogeneously disordered Ge spacer, the ground state for $x = 0.9$ corresponds to $\Theta_0 = 135°$, namely to a concentration at which metallic behaviour still characterizes the conductance, while for $x = 1$ and $\Theta > 135$ 'tunnelling' seems to occur (see figure 8). Increasing the Ge concentration further implies that Θ_0 gradually approaches $180°$, which is the ground state $x = 1$ (see also figure 5).

The opposite is the case for the heterojunction consisting of 15 inhomogeneously disordered Ge layers: only very close to $x = 1$ does the angle specifying the ground state jump from $90°$ to zero (parallel configuration). Only then does 'tunnelling' appear to occur, whereas, even for $x = 0.98$, metallic behaviour applies in both cases for the whole range of Θ.

Figures 15 and 16 show two minimal switching times $t(\Theta_i, \Theta_j; \mathbf{x}, m)$ in the case of non-collinear ground states, namely $t(\Theta_i, \Theta_0; \mathbf{x}, m)$ and $t(\Theta_0, \Theta_j; \mathbf{x}, m)$ with $\Theta_i = 0$ (parallel configuration), $\Theta_j = 180°$ (antiparallel configuration) and Θ_0 referring to the ground state. Since, in principle, switching occurs between the ground state and a collinear final state, all $t(\Theta_i, \Theta_0; \mathbf{x}, m)$ are negative (see also, in particular,
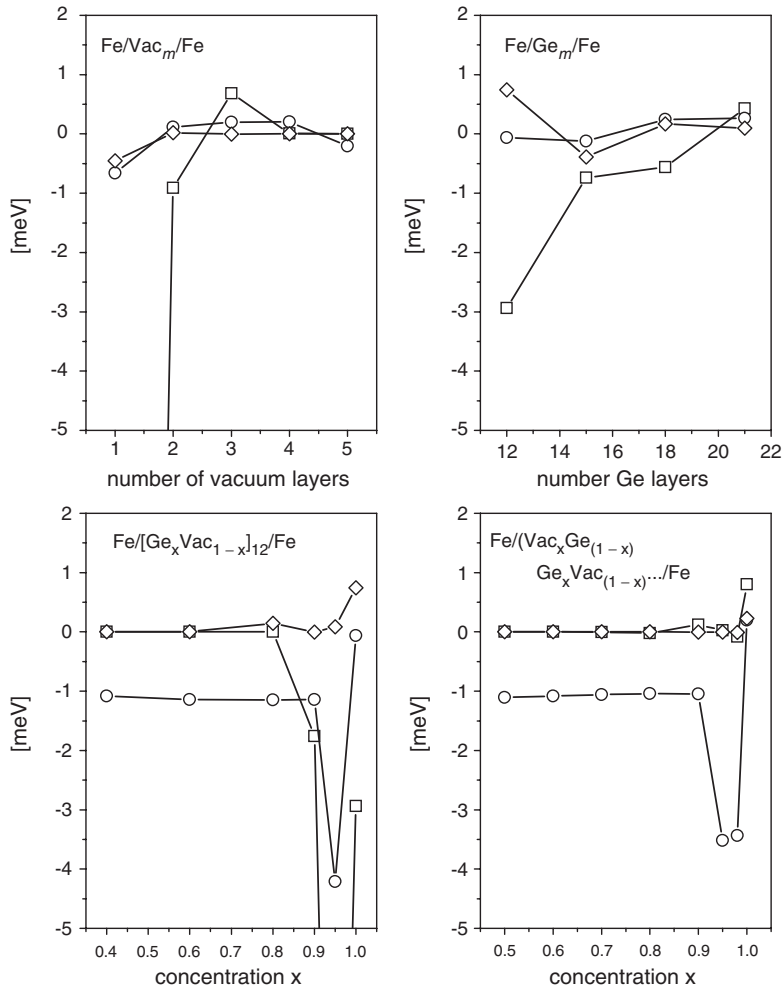
Figure 14. Expansion coefficients $a = -a_1$ (squares), $b = a_2$ (circles) and $c = a_3$ (diamonds) (see also equations (8) and (15)). Note that in order to use the same scale on the ordinate for all investigated cases, for the left column, values less than -5 meV do not appear.

equations (21) and (22)). This is also the reason why the value for $x = 0.95$ is negative in figure 15. It should be recalled that, in the case of the homogeneously disordered spacer for $x > 0.9$, the angle Θ_0 gradually approaches $180°$. Therefore, the representation of this particular point in figure 15 was deliberately chosen so that the transition from a non-collinear ground state to a collinear ground state could best be illustrated. For the inhomogeneously disordered Ge spacer a non-collinear ground state pertains until very close to $x = 1$.

Again, the expansion coefficients for the twisting energy in figure 14 serve as an excellent tool for interpreting the obtained results for the minimal switching times for disordered Ge spacers. In both cases, for $x < 0.9$ a reasonably large (negative) anisotropy term ties the ground state to $\Theta_0 = 90°$ ($|b| \geq |a|$). It should be noted that
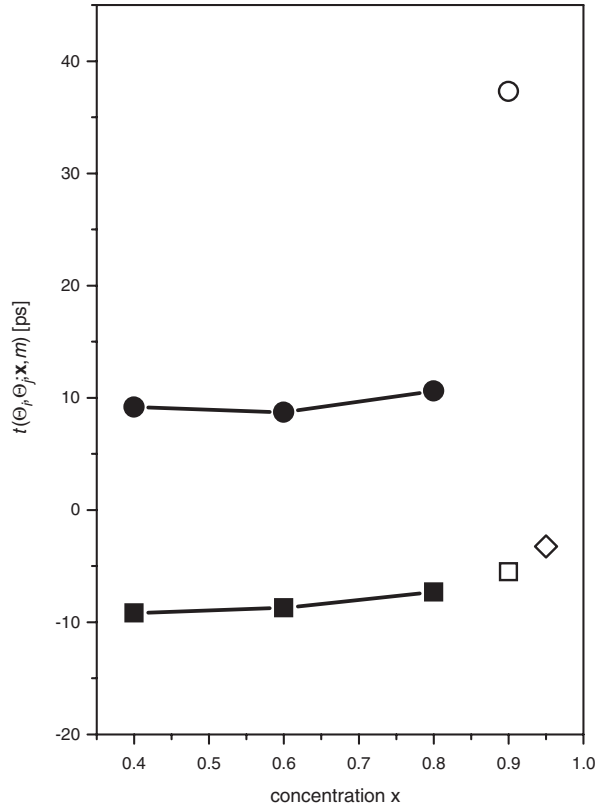
Figure 15. Minimal switching times $t(\Theta_i, \Theta_j; \mathbf{x}, m)$ for the heterojunction consisting of 12 homogeneously alloyed Ge layers. The initial (Θ_i) and final (Θ_i) configurations are indicated, and Θ_0 corresponds to the ground state. Full squares, $\Theta_i = 0°, \Theta_j = \Theta_0 = 90°$; full circles, $\Theta_i = \Theta_0 = 90°, \Theta_j = 180°$; open squares, $\Theta_i = 0°, \Theta_j = \Theta_0 = 130°$; open circles, $\Theta_i = \Theta_0 = 135°, \Theta_j = 180°$; open diamonds, $\Theta_i = 0°, \Theta_j = \Theta_0 = 180°$.

the conditions $b < 0$ and $|b| \geq |a|$ are the actual reason for the occurrence of a non-collinear ground state: the anisotropy term has to be negative and larger than the interlayer exchange term. In both cases the coefficient b has a minimum for $0.9 < x \leq 1$ and is again reasonably small for ordered systems, the position of this minimum being very close to $x = 1$ for the inhomogeneously disordered system. Because the sign of a is different in the two types of disorder, in one case the ground state corresponds to an antiparallel configuration, and in the other to a parallel configuration, which in turn explains the jump in the minimal switching time for the inhomogeneously disordered Ge spacer very close to $x = 1$.

5. Discussion

It would appear that, essentially, two basic concepts can be used to characterize current-induced switching in heterojunctions (at least in those investigated here),
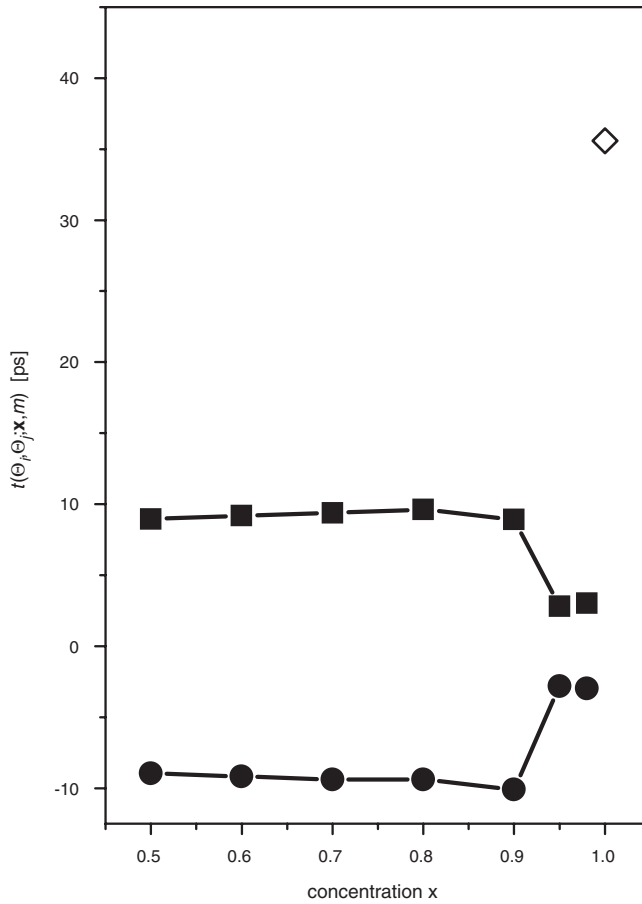
Figure 16. Minimal switching times $t(\Theta_i, \Theta_j; \mathbf{x}, m)$ for the heterojunction consisting of 15 inhomogeneously alloyed Ge layers. The initial (Θ_i) and final (Θ_j) configurations are indicated, and Θ_0 corresponds to the ground state. Full circles, $\Theta_i = 0°$, $\Theta_j = \Theta_0 = 90°$; full squares, $\Theta_i = \Theta_0 = 90°$, $\Theta_j = 180°$; open diamonds, $\Theta_i = 0°$, $\Theta_j = \Theta_0 = 180°$.

namely (1) the analytic properties of the sheet resistance with respect to the imaginary part δ of the Fermi energy, and (2) the size and sign of the expansion coefficients for the twisting energy in a power series in $\cos\Theta$, Θ being the relative angle between the orientations of the magnetization in the magnetic slabs. The Θ dependence of the sheet resistance is perhaps less interesting, because, with the exception of a very few cases, it can be fitted sufficiently accurately using a first-order polynomial in $\cos\Theta$, for example of the form

$$r(\Theta; \mathbf{x}, m) \simeq A(1 - \cos\Theta). \tag{23}$$

In terms of a real space Kubo–Greenwood implementation [21], i.e. in a formulation in which different k-convergence properties at different values of δ cannot

Table 1. Collinear versus non-collinear ground states.

a vs. b	b	Ground state	Θ_0	Θ_1
$\lvert a \rvert \geq \lvert b \rvert$		Collinear	$0°$ or $180°$	$0°$ or $180°$
$\lvert a \rvert \leq \lvert b \rvert$	$b < 0$	Collinear	$0°$ or $180°$	$90°$
	$b > 0$	Non-collinear	$90°$	$0°$ and $180°$

obscure the analytical properties, it was shown that the variation of the sheet resistance is strictly linear with respect to the imaginary part of the Fermi energy. The criterion for distinguishing metallic conductance from tunnelling therefore appears to be very reasonable. It is indeed surprising to discover that, in some systems, the occurrence of 'tunnelling' (see, e.g., figure 4) depends on Θ, which implies that in one collinear configuration metallic conductance can apply, while in another 'tunnelling' is characteristic.

The expansion coefficients a and b for the twisting energy (see equations (8) and (15)) can be used for a rough characterization of the twisting energy and the reduced critical current $I_0(\Theta_1; \mathbf{x}, m)$ (see table 1) in which Θ_0 again specifies the ground state and Θ_1 the reduced critical current. Taking also the third coefficient into account, the shifting of Θ_0 or Θ_1 to values other than $90°$ can be described.

Clearly, in order to be a useful effect, current-induced switching needs to lead to a final state in which the sheet resistance is sufficiently higher than in the initial ground state, or *vice versa*. This is definitely the case if the initial state shows metallic conductance and the final state 'tunnelling', as, for example, in the system Fe/Ge$_m$/Fe (see figure 9). The actual size of the magnetoresistance depends very much on the degree of disorder in the spacer. For $x = 0.9$ in Fe/(Ge$_x$Vac$_{1-x}$)$_{12}$/Fe switching from the ground state at $\Theta_0 = 135$ to the antiparallel final state yields a magnetoresistance of only 1.3%, and to the parallel final state 5.7%. This again shows that, as in all other investigations of enhanced magnetoresistance effects, the crucial problem is the quality of the interfaces (e.g., the presence of interdiffusion, etc.), and, in particular in the case of heterojunctions, also the actual structure of the spacer [6].

Here the effect of structural disorder in the spacer was simulated by considering two kinds of statistically distributed 'holes'. This led to the discovery of non-collinear ground states of the same type as recently described for Py/Cu/Py spin valves with Cu leads [22]. Clearly, current-induced switching seems, in principle, to be feasible in heterojunctions in the same manner as for spin valve systems. The only new feature is the interplay between metallic conductance and 'tunnelling'. The theoretical approach applied not only provides a clear distinction between these two phenomena, but also a rather simple method to characterize twisting energies (and, consequently, also the reduced currents) and switching times in terms of the expansion coefficients of the twisting energy in a power series in the cosine of the relative angle between the orientations of the magnetization in the magnetic slabs. This, however, requires a fully relativistic approach, since only then can the orientation of the magnetization be defined rigorously and, therefore, the anisotropy effects be included properly.

Acknowledgement

References

[1] J. Slonczewski, J. Magn. magn. Mater. **159** L1 (1996).
[2] J. Grollier, P. Boulenc, V. Cros, *et al.*, Appl. Phys. Lett. **83** 509 (2003).
[3] P. Weinberger, V. Drchal, J. Kudrnovsky, *et al.*, Phil. Mag. B **82** 1027 (2002).
[4] P. Weinberger, L. Szunyogh, C. Blaas, *et al.*, Phys. Rev. B **64** 184429 (2001).
[5] H.C. Herper, P. Weinberger, A. Vernes, *et al.*, Phys. Rev. B **64** 184442 (2001).
[6] H. Herper, P. Weinberger, L. Szunyogh, *et al.*, Phys. Rev. B **66** 064426 (2002).
[7] H. Herper, L. Szunyogh, C. Sommers, *et al.*, J. appl. Phys. **91** 8777 (2002).
[8] H.C. Herper, P. Weinberger, L. Szunyogh, *et al.*, J. Magn. magn. Mater. **240** 180 (2002).
[9] E.Y. Tsymbal and D.G. Pettifor, Solid St. Phys. **56** 113 (2001).
[10] P. Weinberger, Phys. Rep. **377** 281 (2003).
[11] P. Weinberger, A. Vernes, B.L. Györffy, *et al.*, Phys. Rev. B **70** 094401 (2004).
[12] P. Weinberger, P.M. Levy, J. Banhart, *et al.*, J. Phys. Condens. Matter **8** 7677 (1996).
[13] J. Zabloudil, R. Hammerling, L. Szunyogh, *et al.*, *Electron Scattering in Solid Matter* (Springer, Heidelberg, 2004).
[14] B. Heinrich, R. Urban and G. Woltersdorf, IEEE Trans. Magn. **38** 2496 (2002).
[15] B. Heinrich, K.B. Urquhart, A.S. Arrott, *et al.*, Phys. Rev. Lett. **59** 1756 (1987).
[16] B. Heinrich, G. Woltersdorf, R. Urban, *et al.*, J. Magn. magn. Mater. **258/259** 376 (2003).
[17] R. Urban, G. Woltersdorf and B. Heinrich, Phys. Rev. Lett. **87** 217204 (2001).
[18] S.H. Vosko, L. Wilk and M. Nusair, Can. J. Phys. **58** 1200 (1980).
[19] H.J.F. Jansen, Phys. Rev. B **59** 4699 (1999).
[20] W.H. Press, B.P. Flannery, S.A. Teukolsky, *et al.*, *Numerical Recipes in Fortran: The Art of Scientific Computing* (Cambridge University Press, Cambridge, 1992).
[21] K. Palotás, B. Lazarovits, L. Szunyogh, *et al.*, Phys. Rev. B **70** 134421 (2004).
[22] A. Vernes, L. Szunyogh and P. Weinberger, Phys. Rev. B in press (2005).